Molecular Imaging of Atherothrombotic Diseases
Seeing Is Believing

Xiaowei Wang, Karlheinz Peter

Abstract—Molecular imaging, with major advances in the development of both innovative targeted contrast agents/particles and radiotracers, as well as various imaging technologies, is a fascinating, rapidly growing field with many preclinical and clinical applications, particularly for personalized medicine. Thrombosis in either the venous or the arterial system, the latter typically caused by rupture of unstable atherosclerotic plaques, is a major determinant of mortality and morbidity in patients. However, imaging of the various thrombotic complications and the identification of plaques that are prone to rupture are at best indirect, mostly unreliable, or not available at all. The development of molecular imaging toward diagnosis and prevention of thrombotic disease holds promise for major advance in this clinically important field. Here, we review the medical need and clinical importance of direct molecular imaging of thrombi and unstable atherosclerotic plaques that are prone to rupture, thereby causing thrombotic complications such as myocardial infarction and ischemic stroke. We systematically compare the advantages/disadvantages of the various molecular imaging modalities, including X-ray computed tomography, magnetic resonance imaging, positron emission tomography, single-photon emission computed tomography, fluorescence imaging, and ultrasound. We further systematically discuss molecular targets specific for thrombi and those characterizing unstable, potentially thrombogenic atherosclerotic plaques. Finally, we provide examples for first theranostic approaches in thrombosis, combining diagnosis, targeted therapy, and monitoring of therapeutic success or failure. Overall, molecular imaging is a rapidly advancing field that holds promise of major benefits to many patients with atherothrombotic diseases.

Visual Overview—An online visual overview is available for this article. **(*Arterioscler Thromb Vasc Biol*. 2017;37:1029-1040. DOI: 10.1161/ATVBAHA.116.306483.)**

Key Words: atherosclerosis ■ coronary artery disease ■ imaging ■ magnetic resonance imaging ■ positron emission tomography ■ thrombosis ■ ultrasound

Cardiovascular disease (CVD) is the leading cause of mortality and morbidity worldwide and represents an immense economic burden.[1] Coronary artery disease and stroke are the most frequent direct causes of death.[2] Arterial thrombosis is the common end point for both coronary artery disease, causing acute myocardial infarction, and cerebrovascular disease, causing stroke. Typically, the underlying disease is atherosclerosis, a chronic inflammatory disease that is usually asymptomatic until unstable atherosclerotic plaques rupture, and thereby trigger the formation of thrombi.[3,4] Molecular imaging, particularly of unstable atherosclerosis and thrombosis, is a rapidly advancing field that has the potential to make a major difference in prevention and therapy and, ultimately, outcome of CVD.[5]

Molecular imaging is a biomedical discipline that enables the visualization, characterization, and quantification of physiological and pathological processes at the whole-body, organ, cellular, and subcellular levels within intact living organisms. This emerging field of research has demonstrated breathtaking progress in the development of many new and innovative biotechnological imaging tools over the past 2 decades. In parallel, impressive advances in imaging technologies have been achieved, with a wide spectrum of modalities now available for clinical and preclinical imaging, progress that has been made possible through a remarkable cross-disciplinary collaboration of chemists, physicists, biologists, and physicians working hand in hand on the development of novel imaging technologies and innovative imaging agents. Molecular imaging promotes the establishment of personalized medicine, the successful implementation of which we are already witnessing in the field of cancer treatment. This review focuses on new developments and the enormous potential offered by molecular imaging for patients with CVD, particularly those with atherosclerotic or thrombotic diseases.

Molecular imaging goes beyond the anatomy of the respective disease and provides additional functional characterization of disease states using specific functional imaging probes. It is based on often complex but rapidly advancing technologies which typically require several components: (1) a solid understanding of biomarkers and their relevance in disease; (2) an in-depth knowledge of imaging contrast agents, their pharmacokinetic properties, and the chemistry required

Received on: December 21, 2016; final version accepted on: April 11, 2017.

From the Atherothrombosis and Vascular Biology Laboratory, Baker Heart and Diabetes Institute (X.W., K.P.), Departments of Medicine (X.W., K.P.), and Immunology (K.P.), Monash University, Melbourne, Victoria, Australia.

Correspondence to Karlheinz Peter, MD, PhD, Atherothrombosis and Vascular Biology, Baker Heart and Diabetes Institute, 75 Commercial Rd, Melbourne, VIC 3004, Australia. E-mail karlheinz.peter@bakeridi.edu.au

Nonstandard Abbreviations and Acronyms	
ApoE	apolipoprotein E
CVD	cardiovascular disease
CT	computed tomography
FI	fluorescence imaging
GPVI	glycoprotein VI
LDL	low-density lipoprotein
MMP	matrix metalloproteinase
MRI	magnetic resonance imaging
NIR	near-infrared
PET	positron emission tomography
RGD	arginine–glycine–aspartic acid
scFv	single-chain antibody
SPECT	single-photon emission computed tomography
SPIO	superparamagnetic iron oxide
VCAM-1	vascular cell adhesion molecule 1

for their conjugation; and (3) the skilled application of high-end imaging equipment to achieve optimal resolution, sensitivity, and real-time imaging. However, these efforts are well rewarded by providing early detection of diseases before the manifestation of clinical symptoms, the ability to follow disease progression or regression over time, and the unique capability to monitor the efficacy of therapy.

We present a brief overview of the clinical need to image atherothrombotic diseases, discuss potential molecular targets, and compare the various molecular imaging modalities, including computed tomography (CT), magnetic resonance imaging (MRI), positron emission tomography (PET), single-photon emission computed tomography (SPECT), fluorescence imaging (FI), bioluminescence imaging, and ultrasound.

Major Clinical Need for Imaging of Atherothrombotic Disease

Thrombotic diseases such as myocardial infarction, ischemic stroke, pulmonary embolism, and deep vein thrombosis are presenting major challenges in clinical medicine.[6] Currently, the diagnosis is mainly based on indirect detection via reduction of flow in the respective vessels. A direct visualization of thrombi through molecular imaging via several possible modalities would increase the reliability and rapidness of diagnosis, and, ultimately, substantially improve the clinical outcome of thrombotic disease. Similarly, the identification of rupture-prone plaques that are associated with an increased risk of thrombotic occlusion is a highly sought-after imaging capability that indeed has often been called the "holy grail of cardiology".

Imaging Modalities

Several imaging platforms are used for molecular imaging. Some are already being used in current clinical practice and contributing to clinical decision-making, whereas others are currently at advanced development stages.[7–9] Although each of these imaging modalities has its own strengths and weaknesses (Table), they are often complementary to one another and hence lead to the development of multimodality and hybrid imaging.

X-ray–based CT has been used for imaging of anatomic structures based on its short scanning time and its high spatial resolution. Invasive coronary angiography, based on the use of a radio-opaque contrast agent and X-rays, is the current gold standard for the diagnosis of coronary artery disease. Recently, coronary CT angiograms have become increasingly used as a gatekeeper for further invasive diagnostic procedures, particularly coronary angiograms.[10] However, CT exposes patients to ionizing radiation. In comparison, MRI incorporates high spatial and temporal resolution, thereby providing excellent soft-tissue contrast and functional imaging capabilities with no requirement of radiation; however, the scanning time needed for an MRI can be lengthy, and its noise level is sometimes irritating for patients. The cost is substantial and patients have to remain still, as even slight movement can reduce image quality. Only a small number of contrast agents are available and patients with certain metallic implants are not able to use this imaging modality. In addition, patients frequently feel claustrophobic in MRI scanners.

PET provides high sensitivity with relatively limited spatial resolution; however, PET imaging relies on radiotracer handling and production in a cyclotron, and scans are usually expensive. To include detailed structural information, PET is often applied in a hybrid approach with CT imaging. However, the combination of PET and CT comes with the concern of radiation safety. Most recently, the hybrid approach of PET and MRI has become highly attractive based on technical advances in the development of positron detectors that can be used in MRI scanners. Another limitation of PET is the short half-life of the PET tracers that are currently used clinically. Although this might not be an issue for conventional, nontargeted imaging, the additional time needed for bioconjugation to ligands has to be taken into account and therefore a targeted molecular imaging approach may be limited by time constraints. However, newer developments of PET tracers and local devices for PET tracer production have the potential to overcome this disadvantage. SPECT technology has similar properties to PET, but it comes with slightly lower cost and higher general availability. The tracers for SPECT also have a longer half-life when compared with those of PET.

Ultrasound imaging is a low-cost modality, with scanners generally available in hospitals and many outpatient settings. Newer generations of ultrasound scanners are also highly portable compared with most other imaging technologies, which enables imaging to be performed at the bedside, in emergency situations, or outside of hospitals. Ultrasound is real-time, has high temporal resolution, and does not involve ionizing radiation; however, ultrasound has restricted depth penetration and is operator dependent. The prototypical contrast agent for ultrasound imaging is microbubbles, which are already Food and Drug Administration approved.

In addition to these established modalities, other highly promising imaging platforms are currently being used in preclinical small-animal imaging, but are still under development for molecular imaging in patients. The most promising is optical imaging, which offers low cost, obviates radiation,

Table. Characterization of Current Noninvasive Molecular Imaging Modalities

Technique	Spatial Resolution, mm	Depth	Acquisition Time	Quantitative	Imaging Agents	Sensitivity of Agents, mol/L	Translation into the Clinic
CT	0.02–0.3 (micro-CT) 0.5–2 (clinical)	Not limited	s– min	Yes	Iodinated molecules	$\approx 10^{-9}$ to 10^{-12}	Yes
MRI	0.01–0.1 (preclinical) 1–1.5 (clinical)	Not limited	min–h	Yes	Gd-chelates, superparamagnetic nanoparticles (SPIO, USPIO, and VSOP)	$\approx 10^{-3}$ to 10^{-5}	Yes
PET	1–2 (micro-PET) 6–10 (clinical)	Not limited	min–h	Yes	^{11}C, ^{18}F, ^{64}Cu, ^{68}Ga, ^{89}Zr radiotracers	$\approx 10^{-10}$ to 10^{-12}	Yes
SPECT	0.5–2 (micro-SPECT) 7–15 (clinical)	Not limited	min–h	Yes	^{99m}Tc, $^{23/124/125/131}$I, ^{111}In radiotracers	$\approx 10^{-10}$ to 10^{-11}	Yes
CEU	0.03–0.1 (preclinical) 0.15–1 (clinical)	cm	s–min	Yes	Microbubbles	Individual	Yes
OI	0.05	cm	min–h	Yes	NIR dyes	$\approx 10^{-9}$ to 10^{-12}	Experimental only
FMT	1	cm	min	Yes	NIR dyes	$\approx 10^{-9}$ to 10^{-12}	Experimental only
BLI	2–5	cm	min	No	Luciferins	$\approx 10^{-15}$ to 10^{-17}	Experimental only

BLI indicates bioluminescence imaging; CEU, contrast-enhanced ultrasound; CT, computed tomography; FMT, fluorescence molecular tomography; Gd, gadolinium; MRI, magnetic resonance imaging; NIR, near infrared; OI, optical imaging; PET, positron emission tomography; SPECT, single-photon emission computed tomography; SPIO, superparamagnetic iron oxide; USPIO, ultrasmall superparamagnetic iron oxide; and VSOP, very small iron oxide particle.

and is highly versatile based on its simultaneous multispectral recording and high resolution. But this modality is so far limited by the low depth penetration of light through tissues, and, therefore, for cardiovascular applications, the accessibility of arteries deep in the tissue/body is a major challenge, at least with the currently available technology. This type of application would require invasive (catheter based) approaches. Nevertheless, both fluorescence molecular tomography and bioluminescence imaging provide efficient, low-cost imaging which is fast and sensitive. However, further technical advances are necessary to overcome the current restriction to low depth penetration.

Most recently, photoacoustic imaging has developed into a highly promising molecular imaging technology. In this modality, short pulses of light are absorbed in the tissue, creating ultrasonic waves that are received by ultrasound transducers, thereby converting light into sound.

Molecular Imaging of Thrombus Components

Thrombosis, in general, is an ideal pathology to be diagnosed by molecular imaging. Thrombi expose numerous epitopes that are specific and not existent on other tissues; these include activated coagulation factors, the end product of the coagulation pathway, which is fibrin, as well as various epitopes on activated platelets.

Currently, there is a lack of targeting tools for coagulation factors such as peptides that specifically recognize activated coagulation factors and antibodies that reliably discriminate between circulating zymogens (proenzymes) and activated coagulation factors. This has hindered the broader application of coagulation factors as targets in molecular imaging. Jaffer et al[11] coupled a peptide that specifically binds to activated factor XIII to a near-infrared (NIR) FI agent and showed its binding specificity in thrombi in vivo via intravital microscopy. Chen et al[12] also demonstrated, in a mouse model of silent brain ischemia, that factor XIII targeting enabled imaging of clotting activity using SPECT/CT.

Fibrin

Fibrin is a frequently used target epitope for molecular imaging. Botnar et al[13] demonstrated the successful use of a small, fibrin-binding, gadolinium-labeled peptide derivative for targeted MRI of thrombosis after atherosclerotic plaque rupture in a rabbit model. Oliveira et al[14] showed a specific uptake of a fibrin-binding peptide conjugated to different radiotracers (^{68}Ga, ^{111}In, or ^{99m}Tc) via multimodal SPECT/PET/CT imaging in a thrombotic rat model. In addition, Blasi et al[15] demonstrated, using the same fibrin-binding peptide conjugated to ^{64}Cu, that a single whole-body PET scan is feasible for the detection of multisite thrombi. The fibrin-specific contrast agent EP-2104R conjugated to gadolinium has been used for the visualization of acute coronary, cardiac, and pulmonary thrombi in MRI.[16–18] A dual PET/MRI using EP-2104R and ^{64}Cu also allowed visualization of thrombi in the carotid artery of rats.[19] The use of EP-2104R has advanced to an initial phase II trial in humans with thrombi in the left ventricle, left/right atrium, thoracic aorta, or carotid artery on a 1.5-T MRI.[20] The group concluded that there was localization of contrast at the thrombus; furthermore, there were no major adverse events.[20] More recently, the same fibrin-binding peptide labeled with the PET-tracer ^{64}Cu successfully imaged thrombosis and clot dissolution after treatment with fibrinolytic agents.[21] Ciesienski et al[22] have also worked on a new fibrin-targeting probe for PET imaging and shown success in detection of arterial thrombi. Using optical coherence tomography, Hara et al used a fibrin-targeted NIR fluorescence agent to image fibrin that was overlying stent struts, comparing bare-metal stents and drug-eluting stents.[23] Using a fibrin-targeting peptide (cysteine–arginine–glutamic acid–lysine–alanine) conjugated onto fluorophore-labeled superparamagnetic iron oxide

(SPIO) particles, Song et al[24] successfully imaged a rat model of myocardial ischemia–reperfusion with both MRI and FI.

Activated Platelets

Besides fibrin, activated platelets are the other most abundant and specific target for molecular imaging of thrombi. Various epitopes on the platelet surface have been targeted, although the number of target epitopes and their specificity for activated platelets vary strongly. Targeting of P-selectin, which is mobilized from alpha granules to the platelet surface membrane upon platelet activation, allows discrimination of activated versus nonactivated platelets. However, P-selectin is not specific for platelets and is also expressed on macrophages, as well as endothelial cells, which limits its suitability as a target epitope for molecular imaging of activated platelets in thrombi. Nevertheless, using fucoidan, a polysaccharidic ligand of P-selectin, Suzuki et al[25] demonstrated that the relative abundance of P-selectin on thrombi was sufficient to allow strong binding of fucoidan-coupled ultra small SPIO particles to thrombi, as directly shown in electron microscopy, and it can be used for imaging of intraluminal thrombi in MRI. Using P-selectin targeted microbubbles, Davidson et al[26] were able to visualize enhanced ultrasound signals in the postischemic region after left anterior descending coronary artery ischemia–reperfusion injury in mice. This technology was further shown to detect myocardial ischemia in nonhuman primates.[27] Using this method, other probes, such as tetrasaccharide ligand sialyl Lewis X[28] and E-selectin,[29] have also been proven to be successful in imaging of cardiac ischemia.

In addition to selectins, several other groups have targeted von Willebrand factor[30,31] and glycoprotein VI (GPVI).[32] Using atherosclerotic murine models, Shim et al[31] showed selective signal enhancement of the aorta using microbubbles targeted to the A1 domain of von Willebrand factor on ultrasound imaging. Bigalke et al[33] observed increased uptake of ^{64}Cu-labeled GPVI antibody fragments on exposed subendothelial collagen in apolipoprotein E knock out (ApoE$^{-/-}$) mice on high-fat diet, when compared with healthy mice, using MRI and PET dual imaging. Metzger et al[34] also demonstrated that GPVI-targeted microbubbles bound to the vessel wall of murine atherosclerotic lesions and could be visualized using high-resolution ultrasound.

Activated GPIIb/IIIa

The GPIIb/IIIa receptor (integrin $\alpha_{IIb}\beta_3$, CD41/CD61) is the most abundant receptor on platelets (60 000–80 000 receptors per platelet). It is only expressed on platelets and their precursors and undergoes a conformational change during platelet activation. The combination of high abundance, cell specificity, and the ability to discriminate between activated and nonactivated platelets makes this epitope an ideal target epitope for molecular imaging. Several groups used arginine–glycine–aspartic acid (RGD) analogs, which mimic binding epitopes of GPIIb/IIIa's natural ligand fibrinogen, to perform molecular imaging of thrombi using several modalities, such as ultrasound,[35–39] MRI,[40] PET,[41] and SPECT.[42] However, RGD analogs are ligand mimetics that are not specific for activated platelets; consequently, these peptides bind to all circulating platelets and, in addition, they are not GPIIb/IIIa specific, consequently binding to several other integrins that use RGD interaction sites. Indeed, these peptides are widely used for imaging of the vitronectin receptor (integrin $\alpha_v\beta_3$, CD51/CD61)[43,44] and cancer imaging.[45–47] Other groups have used the antibody fragment abciximab, which binds to GPIIb/IIIa independent of its activation state, and thus binds to all circulating platelets and also cross-reacts with other integrin receptors.[48,49] Abciximab exhibits a strong affinity to the GPIIb/IIIa receptor; as it blocks fibrinogen binding, it inhibits platelet function for several days, which results in an increased risk of bleeding, and thus it may not be an ideal imaging agent.[50,51] Despite these limitations in specificity, the use of RGD peptides and abciximab has been successful in molecular imaging. This can probably be explained by the extremely high abundance of GPIIb/IIIa in the thrombus relative to other competing receptors on other cells and to circulating platelets in blood. Nevertheless, these reports highlight the unique suitability of GPIIb/IIIa for molecular imaging of thrombi.

Single-chain antibodies (scFv) that specifically bind to activated GPIIb/IIIa receptors have been developed and used for the specific targeting of activated platelets in an array of imaging technologies, including MRI,[52–55] PET,[56] SPECT,[57] and ultrasound.[58–60] $scFv_{anti\text{-}GPIIb/IIIa}$ was conjugated to microparticles of iron oxide, and von zur Muhlen et al[52] demonstrated in vivo MRI of activated platelets and its ability to monitor thrombolytic therapy. In a mouse model of nonocclusive coronary artery thrombosis by Duerschmied et al,[54] the authors showed that this approach allowed the molecular MRI of coronary thrombosis. In a myocardial ischemia–reperfusion injury mouse model, von Elverfeldt et al[55] successfully imaged platelet-driven inflammation and late gadolinium enhancement to depict myocardial necrosis in MRI using these scFvs. Using nuclear imaging, these scFvs were conjugated to ^{111}In to demonstrate their high sensitivity in detecting platelet activation in vitro and ex vivo, resulting in a significant increase in the target/background ratio of the injured carotid artery in SPECT-CT.[57] In a similar study using PET, localization of targeted 18F was specific to the thrombus area.[56] In a mouse cardiac ischemia–reperfusion model, the use of scFv-targeted ^{64}Cu allowed the detection of small degrees of ischemia early on, whereas sensitive serological biomarkers did not detect the minimal degrees of ischemia (Figure 1).[61] Using ultrasound imaging, these scFvs conjugated onto microbubbles, allowing for rapid and real-time contrast-enhanced imaging of ferric chloride–induced thrombosis of the carotid artery (Figure 2).[58] These activated GPIIb/IIIa-targeting scFvs can also be used to monitor the success or failure of thrombolysis after the administration of therapeutic agents such as urokinase.[58,59] More recently, in a first in vivo 3-dimensional FI study, our group also demonstrated that activated GPIIb/IIIa-targeted NIR-conjugates facilitated the detection of thrombi in the carotid artery, as well as emboli in the pulmonary artery (Figure 3).[62]

Molecular Imaging of Epitopes That Signal the Risk of Thrombosis

The development of molecular imaging methods that allow identification of atherosclerotic plaques that are prone to rupture, and thereby to develop thrombotic complications, has attracted major interest. Independently of the individual risk factors, atherogenesis typically includes common features

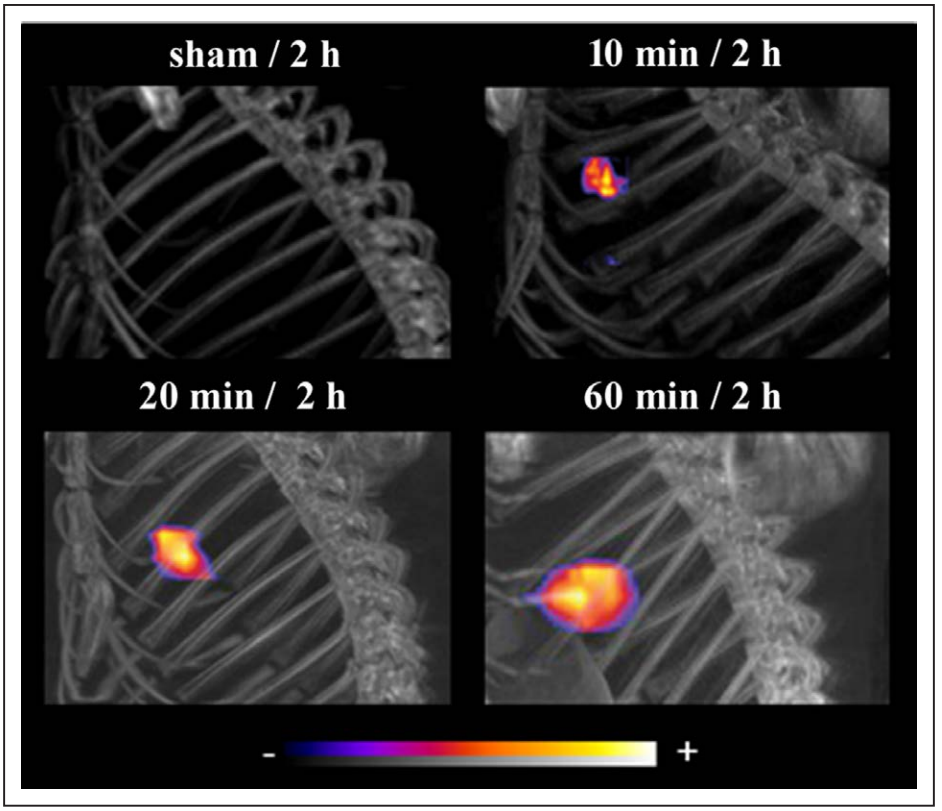

Figure 1. Positron emission tomographic imaging using activated glycoprotein IIb (GPIIb)/IIIa–targeted radiotracers in a cardiac ischemia/reperfusion mouse model. Reproduced from Ziegler et al[61] with permission. Copyright © 2016, The Authors. No radioactivity in the heart was detected after the injection of activated GPIIb/IIIa-targeted ^{64}Cu in sham-operated mice. Specific binding of GPIIb/IIIa-targeted ^{64}Cu was imaged 2 hours after different degrees of ischemia (10, 20, and 60 minutes).

such as inflammatory changes in endothelial cells, subendothelial retention of cholesterol and associated plasma lipoprotein, and accumulation of inflammatory cells.[3] The common final development of plaque instability is particularly associated with distinctive biological processes that can potentially be used as markers of plaque instability and risk for arterial thrombosis. The inflammatory markers on endothelial cells are potentially suitable as targeting epitopes for molecular imaging include vascular cell adhesion molecule 1 (VCAM-1), intercellular adhesion molecule-1, platelet endothelial cellular adhesion molecule, E-selectin, L-selectin, and P-selectin.[63–65]

VCAM-1 and Intercellular Adhesion Molecule-1

VCAM-1 is an endothelial-specific adhesion molecule that is strongly upregulated upon activation of endothelial cells. Atherosclerotic plaques are typically lined with endothelial cells strongly expressing VCAM-1 on their surfaces. Therefore, numerous groups have targeted this particular cell-adhesion molecule as their choice for molecular imaging of atherosclerosis.[66–69] Nahrendorf et al[66] used phage display and identified a peptide mimicking the VCAM-1–binding partner very late antigen-4 to targeted VCAM-1. The authors conjugated this peptide to magnetofluorescent nanoparticles and visualized lesions in ApoE$^{-/-}$ mice using both MRI and optical imaging. Using PET/CT imaging with 18F-labeled tetrametric peptide-targeting VCAM-1, Nahrendorf et al[70] showed in vivo binding of atherosclerotic lesions that correlated to histology and VCAM-1 RNA levels. In a recent study, Bala et al[71] also demonstrated successful imaging of inflamed atherosclerosis plaques using VCAM-1 targeting nanobodies. Kaufmann et al[67] performed contrast-enhanced ultrasound imaging using a monoclonal IgG_1 against VCAM-1 coupled with biotinylated lipid-shelled decafluorobutane microbubbles; their study showed selective signal enhancement of these VCAM-1–targeted microbubbles in the aortas of atherosclerotic mice. This signal increment clearly correlated with the extent of atherosclerosis.[67] Peptides derived from the major histocompatibility complex-1 molecule, which also bind to VCAM-1, were labeled with ^{125}I, ^{123}I, and ^{99m}Tc and successfully used to image atherosclerotic plaques.[68] *Ex vivo* data showed a higher uptake of radioactivity in the aortas of Watanabe heritable hyperlipidemic rabbits when compared with controls.[68] Using MRI, VCAM-1-targeted ultra small SPIOs enabled the visualization of atherosclerotic plaques in mice fed on Western diet.[72] In a recent study using SPECT and FI, Liu et al[73] demonstrated that scFvs directed against VCAM-1, which had been labeled with ^{99m}TC and Cyanine 5 dye, enabled dual-modality detection of atherosclerotic plaques in both mice and rabbits. Another study demonstrated imaging of atherosclerosis using VCAM-1–targeted tobacco mosaic virus in a dual-modal MRI and FI approach.[74] Paulis et al[75] established intercellular adhesion molecule-1–targeted liposomes containing Gd as future MRI agents. Using

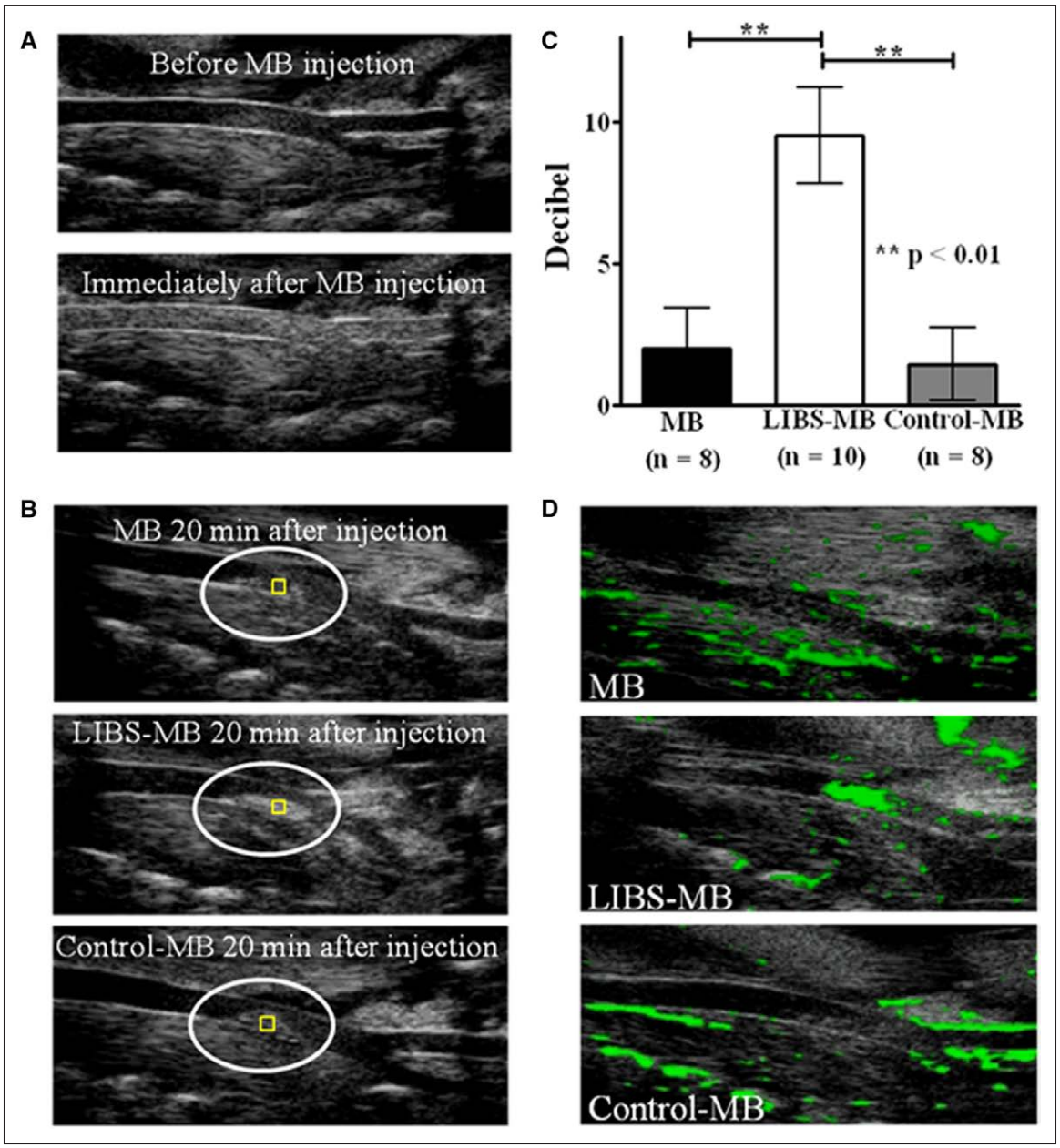

Figure 2. Molecular ultrasound imaging using microbubbles (MBs) targeted to activated glycoprotein IIb/IIIa in vivo in a ferric chloride–induced thrombus. Reproduced from Wang et al[58] with permission. Copyright © 2012, American Heart Association, Inc. **A**, Brightness mode ultrasound images showing the carotid artery before and immediately after the injection of MBs. The carotid artery is a dark lumen before the injection. On MB injection, the vessel lumen becomes a bright and white area. **B**, Real-time brightness mode ultrasound images 20 minutes after the injection of MBs. The dark lumen of the carotid artery shows a light gray area for the thrombus after injection with nonconjugated MBs or nonbinding single-chain antibody control MBs. A white and bright area was seen after the injection of ligand-induced binding site (LIBS)-MBs, where these targeted MBs were attached to the thrombus. **C**, A significant increase in the decibel values was measured for thrombi coated with LIBS-MBs, when compared with MBs or control MBs ($P<0.01$). **D**, Digital subtraction of frames in which areas that are brighter than baseline before the injection of MBs are shown in green. A green thrombus area was observed after the injection of LIBS-MBs, while only nonspecific artifacts were observed for MBs and control MBs.[58]

intercellular adhesion molecule-1–targeted microbubbles, Villanueva et al[76] demonstrated in vitro binding to activated endothelial cells and Demos et al[77] showed in vivo binding to regions of atherosclerotic plaques.

P-Selectin

The adhesion molecule P-selectin (CD62P) is expressed on endothelial cells. Upon their activation, P-selectin is rapidly translocated from the Weibel–Palade bodies to the cell membrane and, as such, is an effective and accessible marker of endothelial cell activation. Kaufmann et al[67] coupled a monoclonal IgG_1 against P-selectin with microbubbles and showed selective ultrasound signal enhancement in the aortas of atherosclerotic mice, demonstrating the suitability of P-selectin as a target for molecular imaging of atherosclerosis. Li et al[78] also demonstrated that 68Ga-labeled fucoidan can be used for

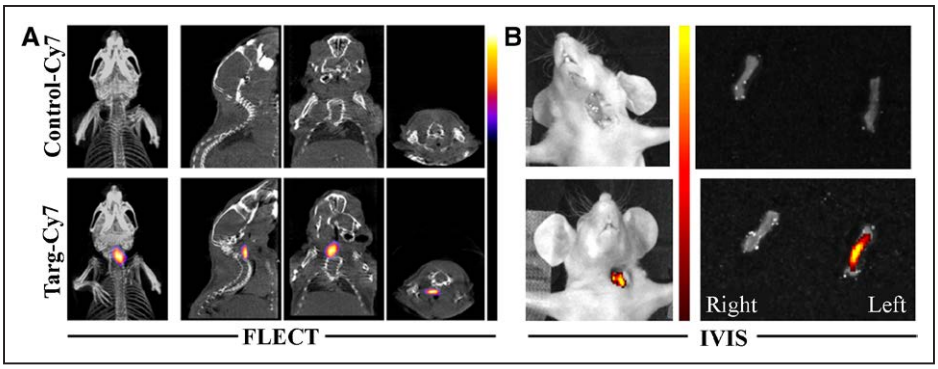

Figure 3. Fluorescence emission computed tomography (FLECT) using an activated glycoprotein IIb/IIIa–targeted near infrared Cy7 dye. Reproduced from Lim et al[62] with permission. Copyright © 2017, The Authors. **A**, In a ferric chloride–induced mouse thrombosis model, targ-Cy7 bound to the thrombus in the left carotid artery and could be imaged via FLECT, while the nonbinding single-chain antibodycontrol-Cy7 did not deliver a specific signal. **B**, Verification of the FLECT signal was performed using the 2-dimensional planar IVIS Lumina scanner after FLECT imaging was completed.

targeting of P-selectin expressed on plaques using PET and showed that their imaging signal correlated with histology, as well as ultrahigh-field MRI.

Vitronectin Receptor $\alpha_v\beta_3$

The vitronectin receptor, integrin $\alpha_v\beta_3$, is a potential marker of endothelial activation, particularly in neovascularization as typically seen in vulnerable atherosclerotic plaques. RGD analogs bind to the vitronectin receptor and thus, this represents a tool for the targeting of activated endothelial cells.[44,79] Using MRI in a rabbit model of atherosclerosis, Winter et al[79] demonstrated increased $\alpha_v\beta_3$ presence within the atherosclerotic wall. Also using RGD peptides (conjugated to ^{99m}Tc), Sun Yoo et al[44] demonstrated a significantly higher uptake of targeted tracers in murine atherosclerotic aortas in SPECT/CT. Using the^{64}Cu PET-labeled, divalent knottin miniprotein, which targets the $\alpha_v\beta_3$ receptor, Jiang et al[80] successfully imaged atherosclerotic lesions in the carotid artery.

Several research groups have also examined the use of dual-targeting contrast agents.[81–83] In vitro experiments investigating the binding of dual-targeted (VCAM-1 and E-selectin) micron-sized iron oxide particles to activated endothelial cells under flow conditions concluded that these particles bound under shear stress and were detectable via optical coherence tomography.[82] Using a dual-targeting iron oxide microparticle (VCAM-1 and P-selectin), McAteer et al[83] identified atherosclerotic changes in mice using ex vivo MRI.

Macrophages and Oxidized Low-Density Lipoprotein

Cellular infiltration and proliferation of inflammatory cells characterize plaques that are prone to rupture and to cause

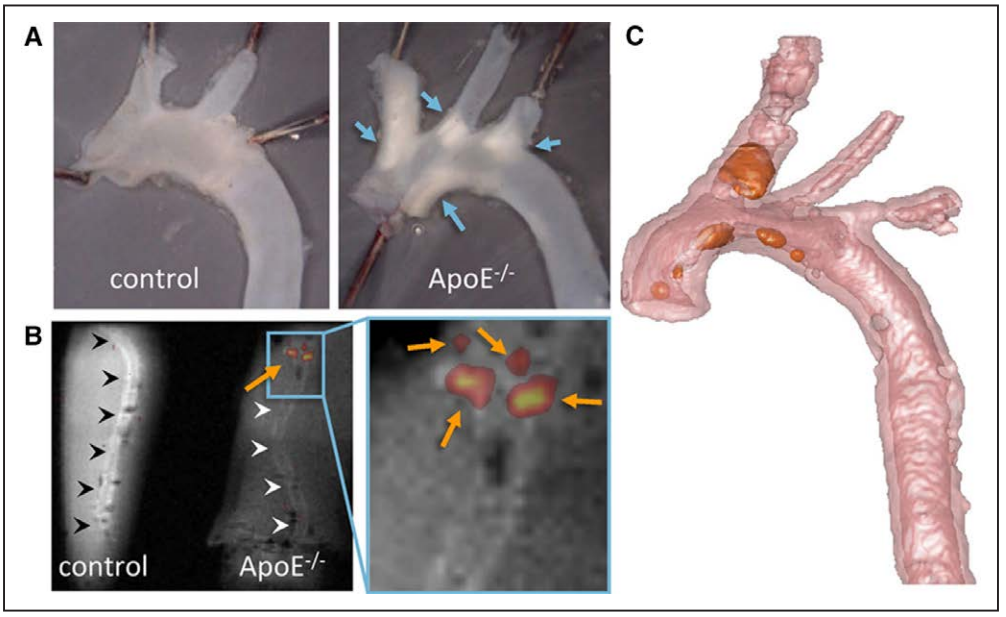

Figure 4 . ^{19}Fluorine magnetic resonance imaging (MRI) of the atherosclerotic plaque in the aortic arches of mice. Reprinted from van Heeswijk et al[86] with permission of the publisher. Copyright © 2015, Radiological Society of North America. **A**, En-face view of aortic arches, showing white patches in the apolipoprotein E (ApoE$^{-/-}$) animals (arrows), but not in the wild-type control. **B**, ^{19}F MRI shows contrast patterns that correlate to the respective en-face photographs. **C**, 3-Dimensional rendering of the aortic arch in pink and ^{19}F contrast signals in orange, showing that the contrast signals are located on the inner surface of the aorta.

thrombotic complications. Macrophages are one of the major inflammatory cells driving atherosclerosis, also playing a key role in the development of plaque instability.[84] As many contrast agents, such as 18F-fluorodeoxyglucose and iron oxide-based nanoparticles (SPIOs and ultra small SPIOs), as well as perfluorocarbon nanoemulsions, undergo phagocytosis by macrophages, these contrast agents accumulate at the site of inflammation and therefore particularly at inflamed, unstable atherosclerotic plaques. Temme et al[85] showed that 19F perfluorocarbon nanoemulsions are taken up by macrophages, thereby enabling imaging of inflammation via MRI. Another study showed 19F perfluorocarbon accumulating at the site of inflammation in atherosclerotic plaques in a mouse model of atherosclerosis (Figure 4).[86] Majmudar et al[87] demonstrated that dextran nanoparticles accumulated in macrophages, thereby enabling the assessment of inflammation in atherosclerotic plaques using PET/MRI.

Macrophages can also be targeted via their surface receptors/markers or their metabolic activity. Tahara et al[88] used 18F-fluorodeoxyglucose to image activated macrophages in atherosclerotic lesions in rabbits in PET imaging. Tarin et al[89] used gold-coated iron oxide nanoparticles conjugated with an anti-CD163 antibody to demonstrate via MRI the targeting of these particles to macrophages in plaques of ApoE$^{-/-}$ mice. The macrophages in atherosclerotic plaques are known to overexpress class A macrophage scavenger receptors, which, in turn, mediate the uptake of modified lipoproteins, such as acetylated and oxidized low-density lipoprotein (LDL). Micelles containing paramagnetic gadolinium–diethylenetriamine pentaacetic acid complexes conjugated to class A macrophage scavenger receptor–specific antibodies showed significant signal enhancement in aortic plaques in vivo in ApoE$^{-/-}$ mice on MRI.[90,91]

Oxidized LDL has long been recognized as a trigger of atherosclerosis. Tsimikas et al[92] demonstrated enrichment of ^{125}I radiotracer coupled to a monoclonal antibody against malondialdehyde–lysine epitopes in oxidized LDL toward atherosclerotic plaques. Using an autoantibody that reacts with malondialdehyde-conjugated LDL labeled with an NIR fluorescence dye on multimodality imaging with fluorescence molecular tomography/CT, Khamis et al[93] demonstrated specific focal accumulation within the aortic arch and its branches in atherosclerotic LDLR$^{-/-}$ mice. Using a scFv directed against oxidized LDL/β2-glycoprotein 1 complexes coupled to ^{64}Cu, Sasaki et al[94] recently observed signal accumulation at the atherosclerotic lesions of Watanabe heritable hyperlipidemic rabbits in PET/CT imaging.

Matrix Metalloproteinases

Matrix metalloproteinases (MMPs), a large family of calcium- and zinc-dependent proteases, play an important role in changes in the vessel scaffold[95]; therefore, MMPs and their activities have been useful targets of unstable plaque for SPECT, MRI, and fluorescence molecular tomography imaging.[96–101] Using ^{99m}Tc-labeled MMP inhibitors, several groups have demonstrated uptake in the atherosclerotic plaque in SPECT imaging, and its correlation with the immunohistochemistry of macrophage infiltration in the vessel.[96,97] By changing the diet of rabbits or placing the animals on statin treatment, Fujimoto et al[97] also showed a reduction in MMP activity. Imaging with microSPECT/CT and using RP782 (an ^{111}In-labeled tracer targeting activated MMPs), Razavian et al[98] demonstrated radioactivity uptake in the aorta and plaque area, as well as a reduction in MMP activity post treatment.

Facilitating Theranostic Approaches

In future, molecular imaging could benefit not only diagnostic approaches but also theranostic approaches, where simultaneous diagnosis and direct disease-targeted therapy can be combined and, in addition, the outcome of the applied treatment can be directly monitored. Targeted delivery of drugs or genes using molecular imaging and their contrast agents provides a beneficial platform for personalized medicine. Several research groups are already working on this cutting-edge approach, showing promising data in the preclinical field of atherosclerosis and thrombosis. Winter et al,[102] following their success in imaging with paramagnetic nanoparticles targeted to the integrin $\alpha_v\beta_3$, loaded their particles with fumagillin and observed decreased MRI signal 7 days post theranostic approach, demonstrating the potential to reduce the plaque burden with these nanoparticles. Using macrophage-targeting iron oxide nanoparticles loaded with NIR dyes and phototoxic agents, McCarthy et al[103] showed that activation by light resulted in the eradication of these macrophages, an approach that may ultimately help to stabilize the unstable plaque. Wang et al[60] have demonstrated that, using dual-targeted microbubbles conjugated to an scFv that is specific for activated GPIIb/IIIa and also a thrombolytic drug, excellent ultrasound visualization of thrombi, successful clot lysis, and success or failure of thrombolytic therapy can be monitored in real time. In addition to conventional drugs, microRNA therapeutics are becoming increasingly popular for theranostic approaches. Kheirolomoon et al[104] used a VCAM-1–targeted cationic liposome for the delivery of anti-miR-712 and demonstrated inhibition of atherosclerosis in mice. Although the theranostic field is relatively new for cardiovascular medicine, substantial technical progress in the development of imaging agents, technical improvements of various imaging modalities, and advances in the development of targeted therapeutics hold strong promise for personalized medicine in patients with CVD.

Future of Molecular Imaging

The clinical translation of molecular imaging has the potential to become an important aspect of the management of CVD, for which diagnostic imaging is already extensively used. Through selecting the correct biomarkers/targeting epitopes and contrast agents, molecular imaging has the ability to diagnose thrombotic diseases, as well as high-risk vulnerable plaques. Molecular imaging will provide a better understanding of disease progress, which will be highly advantageous for the planning and selection of treatment, thereby allowing for individualized and tailored therapy. The different molecular markers expressed at the various stages of disease also facilitate analysis of the treatment efficiency. Further advancement toward a simultaneous theranostic approach will allow a

detailed and informed application of personalized medicine. Overall, the clinical use of molecular imaging has the potential to provide substantial benefits to patients with atherothrombotic disease.

Sources of Funding

X. Wang was supported by a National Heart Foundation of Australia Postdoctoral Fellowship, and K. Peter was supported by a National Health and Medical Research Council Principal Research Fellowship.

Disclosures

K. Peter is inventor of single-chain antibodies targeting glycoprotein IIb/IIIa.

References

1. Laslett LJ, Alagona P Jr, Clark BA 3rd, Drozda JP Jr, Saldivar F, Wilson SR, Poe C, Hart M. The worldwide environment of cardiovascular disease: prevalence, diagnosis, therapy, and policy issues: a report from the American College of Cardiology. *J Am Coll Cardiol*. 2012;60(Suppl 25):S1–49. doi: 10.1016/j.jacc.2012.11.002.
2. Mozaffarian D, Benjamin EJ, Go AS, et al. Heart disease and stroke statistics—2016 update. *Circulation*. 2016;133:e38–e360.
3. Hansson GK, Libby P, Tabas I. Inflammation and plaque vulnerability. *J Intern Med*. 2015;278:483–493. doi: 10.1111/joim.12406.
4. Libby P, Ridker PM, Maseri A. Inflammation and atherosclerosis. *Circulation*. 2002;105:1135–1143.
5. Chen IY, Wu JC. Cardiovascular molecular imaging: focus on clinical translation. *Circulation*. 2011;123:425–443. doi: 10.1161/CIRCULATIONAHA.109.916338.
6. Wendelboe AM, Raskob GE. Global burden of thrombosis: epidemiologic aspects. *Circ Res*. 2016;118:1340–1347. doi: 10.1161/CIRCRESAHA.115.306841.
7. Quillard T, Libby P. Molecular imaging of atherosclerosis for improving diagnostic and therapeutic development. *Circ Res*. 2012;111:231–244. doi: 10.1161/CIRCRESAHA.112.268144.
8. Leuschner F, Nahrendorf M. Molecular imaging of coronary atherosclerosis and myocardial infarction: considerations for the bench and perspectives for the clinic. *Circ Res*. 2011;108:593–606. doi: 10.1161/CIRCRESAHA.110.232678.
9. Wildgruber M, Swirski FK, Zernecke A. Molecular imaging of inflammation in atherosclerosis. *Theranostics*. 2013;3:865–884. doi: 10.7150/thno.5771.
10. Shaw LJ, Hausleiter J, Achenbach S, et al; CONFIRM Registry Investigators. Coronary computed tomographic angiography as a gatekeeper to invasive diagnostic and surgical procedures: results from the multicenter CONFIRM (Coronary CT Angiography Evaluation for Clinical Outcomes: an International Multicenter) registry. *J Am Coll Cardiol*. 2012;60:2103–2114. doi: 10.1016/j.jacc.2012.05.062.
11. Jaffer FA, Tung CH, Wykrzykowska JJ, Ho NH, Houng AK, Reed GL, Weissleder R. Molecular imaging of factor XIIIa activity in thrombosis using a novel, near-infrared fluorescent contrast agent that covalently links to thrombi. *Circulation*. 2004;110:170–176. doi: 10.1161/01.CIR.0000134484.11052.44.
12. Chen JW, Figueiredo JL, Wojtkiewicz GR, Siegel C, Iwamoto Y, Kim DE, Nolte MW, Dickneite G, Weissleder R, Nahrendorf M. Selective factor XIIa inhibition attenuates silent brain ischemia: application of molecular imaging targeting coagulation pathway. *JACC Cardiovasc Imaging*. 2012;5:1127–1138. doi: 10.1016/j.jcmg.2012.01.025.
13. Botnar RM, Perez AS, Witte S, Wiethoff AJ, Laredo J, Hamilton J, Quist W, Parsons EC Jr, Vaidya A, Kolodziej A, Barrett JA, Graham PB, Weisskoff RM, Manning WJ, Johnstone MT. *In vivo* molecular imaging of acute and subacute thrombosis using a fibrin-binding magnetic resonance imaging contrast agent. *Circulation*. 2004;109:2023–2029. doi: 10.1161/01.CIR.0000127034.50006.C0.
14. Oliveira BL, Blasi F, Rietz TA, Rotile NJ, Day H, Caravan P. Multimodal molecular imaging reveals high target uptake and specificity of 111In- and 68Ga-labeled fibrin-binding probes for thrombus detection in rats. *J Nucl Med*. 2015;56:1587–1592. doi: 10.2967/jnumed.115.160754.
15. Blasi F, Oliveira BL, Rietz TA, Rotile NJ, Naha PC, Cormode DP, Izquierdo-Garcia D, Catana C, Caravan P. Multisite thrombus imaging and fibrin content estimation with a single whole-body PET scan in rats. *Arterioscler Thromb Vasc Biol*. 2015;35:2114–2121. doi: 10.1161/ATVBAHA.115.306055.
16. Spuentrup E, Buecker A, Katoh M, Wiethoff AJ, Parsons EC Jr, Botnar RM, Weisskoff RM, Graham PB, Manning WJ, Günther RW. Molecular magnetic resonance imaging of coronary thrombosis and pulmonary emboli with a novel fibrin-targeted contrast agent. *Circulation*. 2005;111:1377–1382. doi: 10.1161/01.CIR.0000158478.29668.9B.
17. Spuentrup E, Fausten B, Kinzel S, Wiethoff AJ, Botnar RM, Graham PB, Haller S, Katoh M, Parsons EC Jr, Manning WJ, Busch T, Günther RW, Buecker A. Molecular magnetic resonance imaging of atrial clots in a swine model. *Circulation*. 2005;112:396–399. doi: 10.1161/CIRCULATIONAHA.104.529941.
18. Overoye-Chan K, Koerner S, Looby RJ, Kolodziej AF, Zech SG, Deng Q, Chasse JM, McMurry TJ, Caravan P. EP-2104R: a fibrin-specific gadolinium-Based MRI contrast agent for detection of thrombus. *J Am Chem Soc*. 2008;130:6025–6039. doi: 10.1021/ja800834y.
19. Uppal R, Catana C, Ay I, Benner T, Sorensen AG, Caravan P. Bimodal thrombus imaging: simultaneous PET/MR imaging with a fibrin-targeted dual PET/MR probe–feasibility study in rat model. *Radiology*. 2011;258:812–820. doi: 10.1148/radiol.10100881.
20. Spuentrup E, Botnar RM, Wiethoff AJ, Ibrahim T, Kelle S, Katoh M, Ozgun M, Nagel E, Vymazal J, Graham PB, Günther RW, Maintz D. MR imaging of thrombi using EP-2104R, a fibrin-specific contrast agent: initial results in patients. *Eur Radiol*. 2008;18:1995–2005. doi: 10.1007/s00330-008-0965-2.
21. Ay I, Blasi F, Rietz TA, Rotile NJ, Kura S, Brownell AL, Day H, Oliveira BL, Looby RJ, Caravan P. *In vivo* molecular imaging of thrombosis and thrombolysis using a fibrin-binding positron emission tomographic probe. *Circ Cardiovasc Imaging*. 2014;7:697–705. doi: 10.1161/CIRCIMAGING.113.001806.
22. Ciesienski KL, Yang Y, Ay I, Chonde DB, Loving GS, Rietz TA, Catana C, Caravan P. Fibrin-targeted PET probes for the detection of thrombi. *Mol Pharm*. 2013;10:1100–1110. doi: 10.1021/mp300610s.
23. Hara T, Ughi GJ, McCarthy JR, Erdem SS, Mauskapf A, Lyon SC, Fard AM, Edelman ER, Tearney GJ, Jaffer FA. Intravascular fibrin molecular imaging improves the detection of unhealed stents assessed by optical coherence tomography in vivo. *Eur Heart J*. 2017;38:447–455.
24. Song Y, Huang Z, Xu J, Ren D, Wang Y, Zheng X, Shen Y, Wang L, Gao H, Hou J, Pang Z, Qian J, Ge J. Multimodal SPION-CREKA peptide based agents for molecular imaging of microthrombus in a rat myocardial ischemia-reperfusion model. *Biomaterials*. 2014;35:2961–2970. doi: 10.1016/j.biomaterials.2013.12.038.
25. Suzuki M, Bachelet-Violette L, Rouzet F, et al. Ultrasmall superparamagnetic iron oxide nanoparticles coated with fucoidan for molecular MRI of intraluminal thrombus. *Nanomedicine (Lond)*. 2015;10:73–87. doi: 10.2217/nnm.14.51.
26. Davidson BP, Kaufmann BA, Belcik JT, Xie A, Qi Y, Lindner JR. Detection of antecedent myocardial ischemia with multiselectin molecular imaging. *J Am Coll Cardiol*. 2012;60:1690–1697. doi: 10.1016/j.jacc.2012.07.027.
27. Davidson BP, Chadderdon SM, Belcik JT, Gupta S, Lindner JR. Ischemic memory imaging in nonhuman primates with echocardiographic molecular imaging of selectin expression. *J Am Soc Echocardiogr*. 2014;27:786–793.e2. doi: 10.1016/j.echo.2014.03.013.
28. Villanueva FS, Lu E, Bowry S, Kilic S, Tom E, Wang J, Gretton J, Pacella JJ, Wagner WR. Myocardial ischemic memory imaging with molecular echocardiography. *Circulation*. 2007;115:345–352. doi: 10.1161/CIRCULATIONAHA.106.633917.
29. Leng X, Wang J, Carson A, Chen X, Fu H, Ottoboni S, Wagner WR, Villanueva FS. Ultrasound detection of myocardial ischemic memory using an E-selectin targeting peptide amenable to human application. *Mol Imaging*. 2014;13:1–9.
30. McCarty OJ, Conley RB, Shentu W, Tormoen GW, Zha D, Xie A, Qi Y, Zhao Y, Carr C, Belcik T, Keene DR, de Groot PG, Lindner JR. Molecular imaging of activated von Willebrand factor to detect high-risk atherosclerotic phenotype. *JACC Cardiovasc Imaging*. 2010;3:947–955. doi: 10.1016/j.jcmg.2010.06.013.
31. Shim CY, Liu YN, Atkinson T, Xie A, Foster T, Davidson BP, Treible M, Qi Y, López JA, Munday A, Ruggeri Z, Lindner JR. Molecular imaging of platelet-endothelial interactions and endothelial von Willebrand factor in early and mid-stage atherosclerosis. *Circ Cardiovasc Imaging*. 2015;8:e002765. doi: 10.1161/CIRCIMAGING.114.002765.
32. Gawaz M, Konrad I, Hauser AI, Sauer S, Li Z, Wester HJ, Bengel FM, Schwaiger M, Schömig A, Massberg S, Haubner R. Non-invasive imaging of glycoprotein VI binding to injured arterial lesions. *Thromb Haemost*. 2005;93:910–913. doi: 10.1160/TH04-10-0660.

33. Bigalke B, Pohlmeyer I, Schönberger T, Griessinger CM, Ungerer M, Botnar RM, Pichler BJ, Gawaz M. Imaging of injured and atherosclerotic arteries in mice using fluorescence-labeled glycoprotein VI-Fc. *Eur J Radiol*. 2011;79:e63–e69. doi: 10.1016/j.ejrad.2011.03.055.
34. Metzger K, Vogel S, Chatterjee M, Borst O, Seizer P, Schönberger T, Geisler T, Lang F, Langer H, Rheinlaender J, Schäffer TE, Gawaz M. High-frequency ultrasound-guided disruption of glycoprotein VI-targeted microbubbles targets atheroprogressison in mice. *Biomaterials*. 2015;36:80–89. doi: 10.1016/j.biomaterials.2014.09.016.
35. Hu G, Liu C, Liao Y, Yang L, Huang R, Wu J, Xie J, Bundhoo K, Liu Y, Bin J. Ultrasound molecular imaging of arterial thrombi with novel microbubbles modified by cyclic RGD *in vitro* and in vivo. *Thromb Haemost*. 2012;107:172–183. doi: 10.1160/TH10-11-0701.
36. Guo S, Shen S, Wang J, Wang H, Li M, Liu Y, Hou F, Liao Y, Bin J. Detection of high-risk atherosclerotic plaques with ultrasound molecular imaging of glycoprotein IIb/IIIa receptor on activated platelets. *Theranostics*. 2015;5:418–430. doi: 10.7150/thno.10020.
37. Schumann PA, Christiansen JP, Quigley RM, McCreery TP, Sweitzer RH, Unger EC, Lindner JR, Matsunaga TO. Targeted-microbubble binding selectively to GPIIb IIIa receptors of platelet thrombi. *Invest Radiol*. 2002;37:587–593. doi: 10.1097/01.RLI.0000031077.17751.B2.
38. Unger E, Porter T, Lindner J, Grayburn P. Cardiovascular drug delivery with ultrasound and microbubbles. *Adv Drug Deliv Rev*. 2014;72:110–126. doi: 10.1016/j.addr.2014.01.012.
39. Rix A, Fokong S, Heringer S, Pjontek R, Kabelitz L, Theek B, Brockmann MA, Wiesmann M, Kiessling F. Molecular ultrasound imaging of αvβ3-integrin expression in carotid arteries of pigs after vessel injury. *Invest Radiol*. 2016;51:767–775. doi: 10.1097/RLI.0000000000000282.
40. Klink A, Lancelot E, Ballet S, Vucic E, Fabre JE, Gonzalez W, Medina C, Corot C, Mulder WJ, Mallat Z, Fayad ZA. Magnetic resonance molecular imaging of thrombosis in an arachidonic acid mouse model using an activated platelet targeted probe. *Arterioscler Thromb Vasc Biol*. 2010;30:403–410. doi: 10.1161/ATVBAHA.109.198556.
41. Kang CM, Koo HJ, An GI, Choe YS, Choi JY, Lee KH, Kim BT. Hybrid PET/optical imaging of integrin αVβ3 receptor expression using a (64) Cu-labeled streptavidin/biotin-based dimeric RGD peptide. *EJNMMI Res*. 2015;5:60. doi: 10.1186/s13550-015-0140-0.
42. Zhou Y, Chakraborty S, Liu S. Radiolabeled cyclic RGD peptides as radiotracers for imaging tumors and thrombosis by SPECT. *Theranostics*. 2011;1:58–82.
43. Golestani R, Mirfeizi L, Zeebregts CJ, Westra J, de Haas HJ, Glaudemans AW, Koole M, Luurtsema G, Tio RA, Dierckx RA, Boersma HH, Elsinga PH, Slart RH. Feasibility of [18F]-RGD for ex vivo imaging of atherosclerosis in detection of αvβ3 integrin expression. *J Nucl Cardiol*. 2015;22:1179–1186. doi: 10.1007/s12350-014-0061-8.
44. Yoo JS, Lee J, Jung JH, Moon BS, Kim S, Lee BC, Kim SE. SPECT/CT Imaging of High-Risk Atherosclerotic Plaques using Integrin-Binding RGD Dimer Peptides. *Sci Rep*. 2015;5:11752. doi: 10.1038/srep11752.
45. Withofs N, Signolle N, Somja J, Lovinfosse P, Nzaramba EM, Mievis F, Giacomelli F, Waltregny D, Cataldo D, Gambhir SS, Hustinx R. 18F-FPRGD2 PET/CT imaging of integrin αvβ3 in renal carcinomas: correlation with histopathology. *J Nucl Med*. 2015;56:361–364. doi: 10.2967/jnumed.114.149021.
46. Melemenidis S, Jefferson A, Ruparelia N, Akhtar AM, Xie J, Allen D, Hamilton A, Larkin JR, Perez-Balderas F, Smart SC, Muschel RJ, Chen X, Sibson NR, Choudhury RP. Molecular magnetic resonance imaging of angiogenesis *in vivo* using polyvalent cyclic RGD-iron oxide microparticle conjugates. *Theranostics*. 2015;5:515–529. doi: 10.7150/thno.10319.
47. Alonso A, Dempfle CE, Della Martina A, Stroick M, Fatar M, Zohsel K, Allémann E, Hennerici MG, Meairs S. *In vivo* clot lysis of human thrombus with intravenous abciximab immunobubbles and ultrasound. *Thromb Res*. 2009;124:70–74. doi: 10.1016/j.thromres.2008.11.019.
48. Coller BS. Binding of abciximab to alpha V beta 3 and activated alpha M beta 2 receptors: with a review of platelet-leukocyte interactions. *Thromb Haemost*. 1999;82:326–336.
49. Schwarz M, Nordt T, Bode C, Peter K. The GP IIb/IIIa inhibitor abciximab (c7E3) inhibits the binding of various ligands to the leukocyte integrin Mac-1 (CD11b/CD18, alphaMbeta2). *Thromb Res*. 2002;107:121–128.
50. Lele M, Sajid M, Wajih N, Stouffer GA. Eptifibatide and 7E3, but not tirofiban, inhibit alpha(v)beta(3) integrin-mediated binding of smooth muscle cells to thrombospondin and prothrombin. *Circulation*. 2001;104:582–587.
51. Peter K, Kohler B, Straub A, Ruef J, Moser M, Nordt T, Olschewski M, Ohman ME, Kübler W, Bode C. Flow cytometric monitoring of glycoprotein IIb/IIIa blockade and platelet function in patients with acute myocardial infarction receiving reteplase, abciximab, and ticlopidine: continuous platelet inhibition by the combination of abciximab and ticlopidine. *Circulation*. 2000;102:1490–1496.
52. von zur Muhlen C, von Elverfeldt D, Moeller JA, Choudhury RP, Paul D, Hagemeyer CE, Olschewski M, Becker A, Neudorfer I, Bassler N, Schwarz M, Bode C, Peter K. Magnetic resonance imaging contrast agent targeted toward activated platelets allows *in vivo* detection of thrombosis and monitoring of thrombolysis. *Circulation*. 2008;118:258–267. doi: 10.1161/CIRCULATIONAHA.107.753657.
53. von zur Muhlen C, Peter K, Ali ZA, Schneider JE, McAteer MA, Neubauer S, Channon KM, Bode C, Choudhury RP. Visualization of activated platelets by targeted magnetic resonance imaging utilizing conformation-specific antibodies against glycoprotein IIb/IIIa. *J Vasc Res*. 2009;46:6–14. doi: 10.1159/000135660.
54. Duerschmied D, Meißner M, Peter K, Neudorfer I, Roming F, Zirlik A, Bode C, von Elverfeldt D, von Zur Muhlen C. Molecular magnetic resonance imaging allows the detection of activated platelets in a new mouse model of coronary artery thrombosis. *Invest Radiol*. 2011;46:618–623. doi: 10.1097/RLI.0b013e31821e62fb.
55. von Elverfeldt D, Maier A, Duerschmied D, et al. Dual-contrast molecular imaging allows noninvasive characterization of myocardial ischemia/reperfusion injury after coronary vessel occlusion in mice by magnetic resonance imaging. *Circulation*. 2014;130:676–687. doi: 10.1161/CIRCULATIONAHA.113.008157.
56. Ardipradja K, Yeoh SD, Alt K, O'Keefe G, Rigopoulos A, Howells DW, Scott AM, Peter K, Ackerman U, Hagemeyer CE. Detection of activated platelets in a mouse model of carotid artery thrombosis with 18 F-labeled single-chain antibodies. *Nucl Med Biol*. 2014;41:229–237. doi: 10.1016/j.nucmedbio.2013.12.006.
57. Heidt T, Deininger F, Peter K, Goldschmidt J, Pethe A, Hagemeyer CE, Neudorfer I, Zirlik A, Weber WA, Bode C, Meyer PT, Behe M, von Zur Mühlen C. Activated platelets in carotid artery thrombosis in mice can be selectively targeted with a radiolabeled single-chain antibody. *PLoS One*. 2011;6:e18446. doi: 10.1371/journal.pone.0018446.
58. Wang X, Hagemeyer CE, Hohmann JD, Leitner E, Armstrong PC, Jia F, Olschewski M, Needles A, Peter K, Ahrens I. Novel single-chain antibody-targeted microbubbles for molecular ultrasound imaging of thrombosis: validation of a unique noninvasive method for rapid and sensitive detection of thrombi and monitoring of success or failure of thrombolysis in mice. *Circulation*. 2012;125:3117–3126. doi: 10.1161/CIRCULATIONAHA.111.030312.
59. Wang X, Palasubramaniam J, Gkanatsas Y, Hohmann JD, Westein E, Kanojia R, Alt K, Huang D, Jia F, Ahrens I, Medcalf RL, Peter K, Hagemeyer CE. Towards effective and safe thrombolysis and thromboprophylaxis: preclinical testing of a novel antibody-targeted recombinant plasminogen activator directed against activated platelets. *Circ Res*. 2014;114:1083–1093. doi: 10.1161/CIRCRESAHA.114.302514.
60. Wang X, Gkanatsas Y, Palasubramaniam J, Hohmann JD, Chen YC, Lim B, Hagemeyer CE, Peter K. Thrombus-targeted theranostic microbubbles: a new technology towards concurrent rapid ultrasound diagnosis and bleeding-free fibrinolytic treatment of thrombosis. *Theranostics*. 2016;6:726–738. doi: 10.7150/thno.14514.
61. Ziegler M, Alt K, Paterson BM, Kanellakis P, Bobik A, Donnelly PS, Hagemeyer CE, Peter K. Highly sensitive detection of minimal cardiac ischemia using positron emission tomography imaging of activated platelets. *Sci Rep*. 2016;6:38161. doi: 10.1038/srep38161.
62. Lim B, Yao Y, Yap M, Huang A, Flierl U, Palasubramaniam J, Wang X, Peter K. A unique three-dimensional fluorescence emission computed tomography technology: in vivo detection of arterial thrombosis and pulmonary embolism. *Theranostics*. 2017;7:1047–1061. doi: 10.7150/thno.18099.
63. Blankenberg S, Barbaux S, Tiret L. Adhesion molecules and atherosclerosis. *Atherosclerosis*. 2003;170:191–203.
64. Ley K, Huo Y. VCAM-1 is critical in atherosclerosis. *J Clin Invest*. 2001;107:1209–1210. doi: 10.1172/JCI13005.
65. Huo Y, Ley K. Adhesion molecules and atherogenesis. *Acta Physiol Scand*. 2001;173:35–43. doi: 10.1046/j.1365-201X.2001.00882.x.
66. Nahrendorf M, Jaffer FA, Kelly KA, Sosnovik DE, Aikawa E, Libby P, Weissleder R. Noninvasive vascular cell adhesion molecule-1 imaging identifies inflammatory activation of cells in atherosclerosis. *Circulation*. 2006;114:1504–1511. doi: 10.1161/CIRCULATIONAHA.106.646380.
67. Kaufmann BA, Sanders JM, Davis C, Xie A, Aldred P, Sarembock IJ, Lindner JR. Molecular imaging of inflammation in atherosclerosis with targeted ultrasound detection of vascular cell adhesion molecule-1. *Circulation*. 2007;116:276–284. doi: 10.1161/CIRCULATIONAHA.106.684738.

68. Broisat A, Riou LM, Ardisson V, Boturyn D, Dumy P, Fagret D, Ghezzi C. Molecular imaging of vascular cell adhesion molecule-1 expression in experimental atherosclerotic plaques with radiolabelled B2702-p. *Eur J Nucl Med Mol Imaging*. 2007;34:830–840. doi: 10.1007/s00259-006-0310-4.
69. Kelly KA, Allport JR, Tsourkas A, Shinde-Patil VR, Josephson L, Weissleder R. Detection of vascular adhesion molecule-1 expression using a novel multimodal nanoparticle. *Circ Res*. 2005;96:327–336. doi: 10.1161/01.RES.0000155722.17881.dd.
70. Nahrendorf M, Keliher E, Panizzi P, Zhang H, Hembrador S, Figueiredo JL, Aikawa E, Kelly K, Libby P, Weissleder R. 18F-4V for PET-CT imaging of VCAM-1 expression in atherosclerosis. *JACC Cardiovasc Imaging*. 2009;2:1213–1222. doi: 10.1016/j.jcmg.2009.04.016.
71. Bala G, Blykers A, Xavier C, Descamps B, Broisat A, Ghezzi C, Fagret D, Van Camp G, Caveliers V, Vanhove C, Lahoutte T, Droogmans S, Cosyns B, Devoogdt N, Hernot S. Targeting of vascular cell adhesion molecule-1 by 18F-labelled nanobodies for PET/CT imaging of inflamed atherosclerotic plaques. *Eur Heart J Cardiovasc Imaging*. 2016;17:1001–1008. doi: 10.1093/ehjci/jev346.
72. Michalska M, Machtoub L, Manthey HD, Bauer E, Herold V, Krohne G, Lykowsky G, Hildenbrand M, Kampf T, Jakob P, Zernecke A, Bauer WR. Visualization of vascular inflammation in the atherosclerotic mouse by ultrasmall superparamagnetic iron oxide vascular cell adhesion molecule-1-specific nanoparticles. *Arterioscler Thromb Vasc Biol*. 2012;32:2350–2357. doi: 10.1161/ATVBAHA.112.255224.
73. Liu C, Zhang X, Song Y, Wang Y, Zhang F, Zhang Y, Zhang Y, Lan X. SPECT and fluorescence imaging of vulnerable atherosclerotic plaque with a vascular cell adhesion molecule 1 single-chain antibody fragment. *Atherosclerosis*. 2016;254:263–270. doi: 10.1016/j.atherosclerosis.2016.09.005.
74. Bruckman MA, Jiang K, Simpson EJ, Randolph LN, Luyt LG, Yu X, Steinmetz NF. Dual-modal magnetic resonance and fluorescence imaging of atherosclerotic plaques *in vivo* using VCAM-1 targeted tobacco mosaic virus. *Nano Lett*. 2014;14:1551–1558. doi: 10.1021/nl404816m.
75. Paulis LE, Jacobs I, van den Akker NM, Geelen T, Molin DG, Starmans LW, Nicolay K, Strijkers GJ. Targeting of ICAM-1 on vascular endothelium under static and shear stress conditions using a liposomal Gd-based MRI contrast agent. *J Nanobiotechnology*. 2012;10:25. doi: 10.1186/1477-3155-10-25.
76. Villanueva FS, Jankowski RJ, Klibanov S, Pina ML, Alber SM, Watkins SC, Brandenburger GH, Wagner WR. Microbubbles targeted to intercellular adhesion molecule-1 bind to activated coronary artery endothelial cells. *Circulation*. 1998;98:1–5.
77. Demos SM, Alkan-Onyuksel H, Kane BJ, Ramani K, Nagaraj A, Greene R, Klegerman M, McPherson DD. *In vivo* targeting of acoustically reflective liposomes for intravascular and transvascular ultrasonic enhancement. *J Am Coll Cardiol*. 1999;33:867–875.
78. Li X, Bauer W, Israel I, Kreissl MC, Weirather J, Richter D, Bauer E, Herold V, Jakob P, Buck A, Frantz S, Samnick S. Targeting P-selectin by gallium-68-labeled fucoidan positron emission tomography for noninvasive characterization of vulnerable plaques: correlation with *in vivo* 17.6T MRI. *Arterioscler Thromb Vasc Biol*. 2014;34:1661–1667. doi: 10.1161/ATVBAHA.114.303485.
79. Winter PM, Caruthers SD, Yu X, Song SK, Chen J, Miller B, Bulte JW, Robertson JD, Gaffney PJ, Wickline SA, Lanza GM. Improved molecular imaging contrast agent for detection of human thrombus. *Magn Reson Med*. 2003;50:411–416. doi: 10.1002/mrm.10532.
80. Jiang L, Tu Y, Kimura RH, Habte F, Chen H, Cheng K, Shi H, Gambhir SS, Cheng Z. 64Cu-labeled divalent cystine knot peptide for imaging carotid atherosclerotic plaques. *J Nucl Med*. 2015;56:939–944. doi: 10.2967/jnumed.115.155176.
81. Ferrante EA, Pickard JE, Rychak J, Klibanov A, Ley K. Dual targeting improves microbubble contrast agent adhesion to VCAM-1 and P-selectin under flow. *J Control Release*. 2009;140:100–107. doi: 10.1016/j.jconrel.2009.08.001.
82. Jefferson A, Wijesurendra RS, McAteer MA, Digby JE, Douglas G, Bannister T, Perez-Balderas F, Bagi Z, Lindsay AC, Choudhury RP. Molecular imaging with optical coherence tomography using ligand-conjugated microparticles that detect activated endothelial cells: rational design through target quantification. *Atherosclerosis*. 2011;219:579–587. doi: 10.1016/j.atherosclerosis.2011.07.127.
83. McAteer MA, Schneider JE, Ali ZA, Warrick N, Bursill CA, von zur Muhlen C, Greaves DR, Neubauer S, Channon KM, Choudhury RP. Magnetic resonance imaging of endothelial adhesion molecules in mouse atherosclerosis using dual-targeted microparticles of iron oxide. *Arterioscler Thromb Vasc Biol*. 2008;28:77–83. doi: 10.1161/ATVBAHA.107.145466.
84. Ley K, Miller YI, Hedrick CC. Monocyte and macrophage dynamics during atherogenesis. *Arterioscler Thromb Vasc Biol*. 2011;31:1506–1516. doi: 10.1161/ATVBAHA.110.221127.
85. Temme S, Jacoby C, Ding Z, Bönner F, Borg N, Schrader J, Flögel U. Technical advance: monitoring the trafficking of neutrophil granulocytes and monocytes during the course of tissue inflammation by noninvasive 19F MRI. *J Leukoc Biol*. 2014;95:689–697. doi: 10.1189/jlb.0113032.
86. van Heeswijk RB, Pellegrin M, Flögel U, Gonzales C, Aubert JF, Mazzolai L, Schwitter J, Stuber M. Fluorine MR imaging of inflammation in atherosclerotic plaque in vivo. *Radiology*. 2015;275:421–429. doi: 10.1148/radiol.14141371.
87. Majmudar MD, Yoo J, Keliher EJ, Truelove JJ, Iwamoto Y, Sena B, Dutta P, Borodovsky A, Fitzgerald K, Di Carli MF, Libby P, Anderson DG, Swirski FK, Weissleder R, Nahrendorf M. Polymeric nanoparticle PET/MR imaging allows macrophage detection in atherosclerotic plaques. *Circ Res*. 2013;112:755–761. doi: 10.1161/CIRCRESAHA.111.300576.
88. Tahara N, Mukherjee J, de Haas HJ, et al. 2-deoxy-2-[18F]fluoro-D-mannose positron emission tomography imaging in atherosclerosis. *Nat Med*. 2014;20:215–219. doi: 10.1038/nm.3437.
89. Tarin C, Carril M, Martin-Ventura JL, Markuerkiaga I, Padro D, Llamas-Granda P, Moreno JA, García I, Genicio N, Plaza-Garcia S, Blanco-Colio LM, Penades S, Egido J. Targeted gold-coated iron oxide nanoparticles for CD163 detection in atherosclerosis by MRI. *Sci Rep*. 2015;5:17135. doi: 10.1038/srep17135.
90. Amirbekian V, Lipinski MJ, Briley-Saebo KC, Amirbekian S, Aguinaldo JG, Weinreb DB, Vucic E, Frias JC, Hyafil F, Mani V, Fisher EA, Fayad ZA. Detecting and assessing macrophages *in vivo* to evaluate atherosclerosis noninvasively using molecular MRI. *Proc Natl Acad Sci U S A*. 2007;104:961–966. doi: 10.1073/pnas.0606281104.
91. Mulder WJ, Jaffer FA, Fayad ZA, Nahrendorf M. Imaging and nanomedicine in inflammatory atherosclerosis. *Sci Transl Med*. 2014;6:239sr1. doi: 10.1126/scitranslmed.3005101.
92. Tsimikas S, Shortal BP, Witztum JL, Palinski W. *In vivo* uptake of radiolabeled MDA2, an oxidation-specific monoclonal antibody, provides an accurate measure of atherosclerotic lesions rich in oxidized LDL and is highly sensitive to their regression. *Arterioscler Thromb Vasc Biol*. 2000;20:689–697.
93. Khamis RY, Woollard KJ, Hyde GD, Boyle JJ, Bicknell C, Chang SH, Malik TH, Hara T, Mauskapf A, Granger DW, Johnson JL, Ntziachristos V, Matthews PM, Jaffer FA, Haskard DO. Near infrared fluorescence (NIRF) molecular imaging of oxidized LDL with an autoantibody in experimental atherosclerosis. *Sci Rep*. 2016;6:21785. doi: 10.1038/srep21785.
94. Sasaki T, Kobayashi K, Kita S, Kojima K, Hirano H, Shen L, Takenaka F, Kumon H, Matsuura E. *In vivo* distribution of single chain variable fragment (scFv) against atherothrombotic oxidized LDL/β2-glycoprotein I complexes into atherosclerotic plaques of WHHL rabbits: Implication for clinical PET imaging. *Autoimmun Rev*. 2017;16:159–167. doi: 10.1016/j.autrev.2016.12.007.
95. Sadeghi MM, Glover DK, Lanza GM, Fayad ZA, Johnson LL. Imaging atherosclerosis and vulnerable plaque. *J Nucl Med*. 2010;51 Suppl 1:51S–65S. doi: 10.2967/jnumed.109.068163.
96. Haider N, Hartung D, Fujimoto S, Petrov A, Kolodgie FD, Virmani R, Ohshima S, Liu H, Zhou J, Fujimoto A, Tahara A, Hofstra L, Narula N, Reutelingsperger C, Narula J. Dual molecular imaging for targeting metalloproteinase activity and apoptosis in atherosclerosis: molecular imaging facilitates understanding of pathogenesis. *J Nucl Cardiol*. 2009;16:753–762. doi: 10.1007/s12350-009-9107-8.
97. Fujimoto S, Hartung D, Ohshima S, et al. Molecular imaging of matrix metalloproteinase in atherosclerotic lesions: resolution with dietary modification and statin therapy. *J Am Coll Cardiol*. 2008;52:1847–1857. doi: 10.1016/j.jacc.2008.08.048.
98. Razavian M, Tavakoli S, Zhang J, Nie L, Dobrucki LW, Sinusas AJ, Azure M, Robinson S, Sadeghi MM. Atherosclerosis plaque heterogeneity and response to therapy detected by *in vivo* molecular imaging of matrix metalloproteinase activation. *J Nucl Med*. 2011;52:1795–1802. doi: 10.2967/jnumed.111.092379.
99. Amirbekian V, Lipinski MJ, Briley-Saebo KC, Amirbekian S, Aguinaldo JG, Weinreb DB, Vucic E, Frias JC, Hyafil F, Mani V, Fisher EA, Fayad ZA. Detecting and assessing macrophages *in vivo* to evaluate atherosclerosis noninvasively using molecular MRI. *Proc Natl Acad Sci U S A*. 2007;104:961–966. doi: 10.1073/pnas.0606281104.
100. Hyafil F, Vucic E, Cornily JC, Sharma R, Amirbekian V, Blackwell F, Lancelot E, Corot C, Fuster V, Galis ZS, Feldman LJ, Fayad ZA.

Monitoring of arterial wall remodelling in atherosclerotic rabbits with a magnetic resonance imaging contrast agent binding to matrix metalloproteinases. *Eur Heart J*. 2011;32:1561–1571. doi: 10.1093/eurheartj/ehq413.
101. Deguchi JO, Aikawa M, Tung CH, Aikawa E, Kim DE, Ntziachristos V, Weissleder R, Libby P. Inflammation in atherosclerosis: visualizing matrix metalloproteinase action in macrophages in vivo. *Circulation*. 2006;114:55–62. doi: 10.1161/CIRCULATIONAHA.106.619056.
102. Winter PM, Neubauer AM, Caruthers SD, Harris TD, Robertson JD, Williams TA, Schmieder AH, Hu G, Allen JS, Lacy EK, Zhang H, Wickline SA, Lanza GM. Endothelial alpha(v)beta3 integrin-targeted fumagillin nanoparticles inhibit angiogenesis in atherosclerosis. *Arterioscler Thromb Vasc Biol*. 2006;26:2103–2109. doi: 10.1161/01.ATV.0000235724.11299.76.
103. McCarthy JR, Korngold E, Weissleder R, Jaffer FA. A light-activated theranostic nanoagent for targeted macrophage ablation in inflammatory atherosclerosis. *Small*. 2010;6:2041–2049. doi: 10.1002/smll.201000596.
104. Kheirolomoom A, Kim CW, Seo JW, Kumar S, Son DJ, Gagnon MK, Ingham ES, Ferrara KW, Jo H. Multifunctional nanoparticles facilitate molecular targeting and miRNA delivery to inhibit atherosclerosis in apolipoprotein E (ApoE$^{-/-}$) mice. *ACS Nano*. 2015;9:8885–8897. doi: 10.1021/acsnano.5b02611.

Highlights

- There is a strong medical need for direct visualization of thrombi and the identification of unstable, rupture-prone atherosclerotic plaques.
- Molecular imaging provides information beyond structure and tissue characterization by targeting of function-specific epitopes.
- Both thrombi and unstable atherosclerotic plaques offer abundant and specific epitopes that can be specifically targeted by molecular imaging.
- Technical advances in scanner technologies and the development of many new and innovative biotechnological imaging tools have resulted in attractive molecular imaging approaches using various imaging modalities, such as ultrasound, positron emission tomography, fluorescence imaging and magnetic resonance imaging.
- The demonstrated and discussed examples of molecular imaging of atherothrombotic diseases highlights not only the potential benefits for diagnostic but also theranostic approaches in cardiovascular diseases.

Arteriosclerosis, Thrombosis, and Vascular Biology

JOURNAL OF THE AMERICAN HEART ASSOCIATION

Molecular Imaging of Atherothrombotic Diseases: Seeing Is Believing

Xiaowei Wang and Karlheinz Peter

Arterioscler Thromb Vasc Biol. 2017;37:1029-1040; originally published online April 27, 2017;
doi: 10.1161/ATVBAHA.116.306483
Arteriosclerosis, Thrombosis, and Vascular Biology is published by the American Heart Association, 7272 Greenville Avenue, Dallas, TX 75231

Print ISSN: 1079-5642. Online ISSN: 1524-4636